Desalination and Water Treatment
www.deswater.com

doi: 10.5004/dwt.2023.29846

307 (2023) 180–189
September

Sequestration of a cationic dye using graphene oxide as adsorbent

Nidhi Rai[a], Sanju Soni[a], Aazad Verma[a], Alok Mittal[b], Richard Baker[c], Syed Ansar Ali Shah[c], Charu Arora[a,*]

[a]*Department of Chemistry, Guru Ghasidas University, Bilaspur-495009, Chhattisgarh, India, emails: charuarora77@gmail.com (C. Arora), needhirai786@gmail.com (N. Rai), aazad.ggvchem@gmail.com (A. Verma)*
[b]*Department of Chemistry, Maulana Azad National Institute of Technology, Bhopal, M.P., India, email: aljymittal@gmail.com*
[c]*School of Chemistry, University of St. Andrews, North Haugh, St. Andrews, Fife, KY16 9ST, U.K., emails: rtb5@st-andrews.ac.uk (R. Baker), saas1@st-andrews.ac.uk (S.A.A. Shah)*

Received 11 June 2023; Accepted 12 August 2023

ABSTRACT

Herein, we reported graphene oxide, as a suitable adsorbent for wastewater treatment to remove crystal violet dye from an aqueous solution. Crystal violet is used for various purposes including colouring, textile, pharmaceuticals etc. It has many harmful effects as it is non-biodegradable, toxic and carcinogenic in nature. So, it is very important to eradicate it from the water. Graphene oxide has been prepared by the modified Hummer's method and characterized by scanning electron microscopy, Fourier-transform infrared spectroscopy and X-ray diffraction. Graphene oxide's removal efficiency depends on various factors including temperature, pH, and substrate concentration. The experimental data from batch studies is well substantiated with pseudo-second-order kinetics with an R^2 value of 0.98 and Temkin adsorption isotherm (R^2: 0.94) with a Temkin constant (b_T) value of 328 kJ/mol. It also closely fits the intraparticle diffusion model (R^2: 0.99). The Langmuir adsorption capacity of graphene oxide was calculated to be 15.87 mg/g. The thermodynamic parameter study suggested that the adsorption process is exothermic and spontaneous in nature. Furthermore, a fixed bed column study was also conducted with a constant flow rate of 2.5 mL/min and bed height of 1 cm with a high concentration of crystal violet in a continuous mode of operation to evaluate its practical applicability and the area under the curve is found to be 4,701 cm^2.

Keywords: Graphene oxide; Organic dye removal; Dye adsorption; Crystal violet; Adsorption characteristics

1. Introduction

Synthetic dyes are widely used in the textile, paper, wood, and cosmetics industries to colour their products. The effluents from textile plants contain a portion of dyes that are classed as pollutants [1,2]. These dyes are deeply coloured and multi-component. They affect aquatic life by absorbing dissolved oxygen from water bodies. In nature, organic dyes are highly carcinogenic and poisonous. Nowadays, many countries face water shortages as most water bodies are contaminated. Dyes are water-soluble and so it is challenging to treat them with chemical or physical methods [3]. Many methods have been developed to treat these organic pollutants including adsorption, coagulation, advanced oxidation, membrane separation, photocatalytic and ozonation from industrial waste [4–9]. Among these, adsorption is the most economical and efficient method reported to date and many materials had been reported to act as adsorbents including coal, wood, rice husk, flash ash, activated carbon, cotton waste, clay, and other porous materials [10–13].

Crystal violet (CV) is a cationic dye that belongs to the class of triphenylmethane dyes and is used for various

* Corresponding author.

purposes such as dermatological drugs, textile colouring, and paper printing though it has many harmful effects as it is non-biodegradable, toxic, mutagenic, and carcinogenic in nature. It also poses a problem for ecosystems because it reduces light transmission and so affects the photosynthetic activity of aquatic organisms. For this reason, it is necessary to remove it from or prevent it from entering the environment.

Graphene oxide (GO) has a 2-D structure and it is an oxidation product of graphene one of the most important allotropes of carbon consisting of a single sheet monolayer of carbon atoms packed into a honeycomb crystal plane. Due to the unique chemical and physical properties of GO such as surface area, high pore volume, presence of surface functionality and its ability to avoid adsorbent aggregation, it has gained immense attention from researchers [14–18]. There is a lot of scope for the development of these materials to enhance their chemical and physical properties by attaching functional groups such as hydroxyl, epoxide, carboxyl, and carbonyl functional groups. These may be hydrophilic or negatively charged, and allow the material to be readily dispersed in water to form a stable colloidal suspension. GO has special qualities like simple combinability with other substances, high specific surface area, and strong heat transfer. Many pollutants, including poisonous colours, arsenic, and 17β-estradiol, have been eliminated using it. GO-based material has been explored for the adsorption of dyes from wastewater. Khan et al. [19,20] has used graphene oxide nanotubes for the adsorption of CV.

The present study aims to explore the application of graphene oxide as a potential adsorbent for the removal of CV. Investigations on the effect of contact time, initial concentration, amount of adsorbent and temperature on the adsorption process have been carried out. Studies have also been carried out to find adsorption isotherm and kinetics of adsorption. The use of pure GO for CV removal is still an unexplored area and it shows far better adsorption capacity than many adsorbents.

2. Material and methods

2.1. Material and apparatus

All chemicals and reagents are commercially available and used as received for synthesis and analysis. CV is a cationic dye used in many industries as a colouring reagent. It was purchased from SCI – Fine Chemicals and used without any further modification. pH of solution was maintained by using HCl (1 N) and NaOH (1 N). X-ray diffraction (XRD) analysis of the samples was carried out using a PANalytical Empyrean diffractometer with $CuK_{\alpha 1}$ monochromatic radiation. The external standard used was high-grade silicon powder which allowed correction for instrumental broadening. Data were acquired at room temperature by scanning 2θ from 10° to 90° with a step size of 0.017° and a step time of 0.95 s. Scanning electron microscopy (SEM) images were obtained on uncoated samples using a JEOL JSM-IT200 instrument equipped with a tungsten filament and operating in secondary electron mode at 15 kV. To analyze the functional groups of the graphene oxide, Fourier-transform infrared spectra were recorded using a Fourier-transform infrared spectroscopy analyzer.

2.2. Preparation of graphene oxide

Graphene oxide was prepared by the modified Hummer method. In this method, additional $KMnO_4$ is added with Hummer's reagent. Concentrated H_2SO_4 (70 mL) was added to a mixture of graphite flakes (2 g, 1 wt. equivalent) and $NaNO_3$ (1.5 g), and the mixture was cooled to 273.15 K using an ice bath. $KMnO_4$ (12.0 g, 3 wt. equivalent) was added in portions while keeping the temperature below 293.15 K. The mixture was stirred in an ice bath for 1.5 h and warmed to 308.15 K for 3 h. Water was added slowly and the solution turned milky golden brown in colour and produced a large exotherm to 371.15 K. External temperature was maintained at 371.15 K by using a water bath. After cooling, the mixture of additional water (300 mL) and 30% H_2O_2 (15 mL) was added after which the colour of the mixture changed to a golden brown. The mixture was centrifuged for 30 min and the supernatant was decanted away. The remaining solid material was then washed with water (300 mL) followed by 30% HCl (300 mL) and after that, it was washed with ethanol (300 mL) twice. After some time, a brown supernatant was obtained. It was dried in an oven for 2 h at 373 K [18].

2.3. Adsorption study procedure

The dye removal study was carried out spectrophotometrically by applying batch and column techniques. A stock solution of CV (50 mg/L) was prepared by dissolving 12.5 mg of CV in 250 mL water. All further solutions were prepared by diluting the stock solution to get the required concentration. To study the adsorption isotherm and kinetics, a fixed amount of graphene oxide was added to a series of 5 mL samples of a diluted solution (2–6 mg/L) of CV dye, and the change in the absorbance peak was observed at the. The wavelength of maximum absorption of the CV dye (λ_{max} = 589 nm). The removal efficiency (%) of graphene oxide and dye uptake capacity, that is, the amount of dye in (mg) adsorbed on the surface per gram of graphene oxide (Q_e) adsorbent was calculated according to the following equations [21].

$$\text{Dye Removal}(\%) = \frac{(C_0 - C_e)}{C_0} \times 100 \tag{1}$$

$$Q_t = \frac{(C_0 - C_t)V}{m} \tag{2}$$

$$Q_e = \frac{(C_0 - C_e)V}{m} \tag{3}$$

where C_0, C_t and C_e (mg/L) are the initial concentration of the dye solution, concentration at time t, and equilibrium concentration, respectively, V (L) is the volume of the dye solution, and m (g) is the mass of adsorbent used. Furthermore, the effect of various parameters such as temperature, adsorbent dose, contact time, pH, and initial concentration of dye was studied [22,23].

2.4. Column adsorption study

The column adsorption study was run in a glass column with 27 cm length, 0.5 cm diameter and containing 0.5 g

of adsorbent. The adsorbent was placed with a fixed bed height of 1 cm and cross-sectional area of 0.2 cm^2 on a cotton wool support. The dye solution of concentration 50 mg/L was added to the column for the experiment. Aliquots of 6.0 mL of effluent solution were collected at regular time intervals of 5 min and observed spectrophotometrically for dye content.

The breakthrough curve was plotted in terms of C_t/C_0 vs. time, where C_0 and C_t have the meanings given above. The volume of effluent V_{ef} can be calculated by using the following formula:

$$V_{ef} = \upsilon t \tag{4}$$

where t (min) is the flow time and υ (mL/min) is the flow rate.

The area under the breakthrough curve represents the amount of dye adsorbed at time t, Q_{total} (mg), and can be determined by integration (calculated using the Software Origin Pro-8).

$$Q_{total} = \upsilon \int_{t=0}^{t=t} \left(C_0 - C_t\right) dt \tag{5}$$

The total mass of dye (m_{total}) added to the column at time t can be calculated by:

$$m_{total} = C_0 \upsilon t \tag{6}$$

The dye removal R (%) can be calculated as:

$$R = \frac{Q_{total}}{m_{total}} \times 100 \tag{7}$$

The adsorption capacity of the adsorbent q_t (mg/g) at time t can be obtained using the following equation (calculated using Software Origin Pro-8).

$$q_t \frac{V \int_{t=0}^{t=t} \left(C_0 - C_t\right) dt}{m} \tag{8}$$

where m is the amount of adsorbent used in the column.

3. Results and discussion

3.1. Characterisation of graphene oxide

In Fig. 1 the Fourier transform infrared spectrum of graphene oxide shows broad peaks all 2,900–3,700 cm^{-1}. The peaks at 2,927 and 2,866 cm^{-1} are due to symmetric and asymmetric vibration of CH_2. The peak at 1,727 and 3,250 cm^{-1} corresponds to the C–O of carboxylic acid and the C–OH group of alcohol, respectively. This confirms the presence of oxygen-containing functional groups, consistent with the oxidation of graphene that has been oxidized. The hydrophilic nature of graphene oxide is due to the formation of hydrogen bonds between graphite and water molecules within the polar hydroxyl groups and the data obtained is in good agreement with recent published papers [24].

The crystalline structure of graphene oxide was analysed by X-ray diffraction and it is shown in Fig. 2. In the figure, the diffraction peak is shown at 2θ = 26.45. The wide peak shows the oxidation of graphite and shows the damage of the regular crystalline pattern graphite during the oxidation. Thus, it suggests the synthesis of GO and a decrease in interlayer spacing. The crystallite size of GO is found to be 16.99 nm from XRD data. The reported data are well-matched with recently published papers [25,26].

The surface morphology of graphene oxide imaged SEM (Fig. 3). The particle size reduction has a significant effect on GO, and the graphite stack splits into layers. Further, the internal layers are more disassembled, and a curly structure is observed. Efficient oxidation during the process is possible due to surface area (due to particle size reduction). Elements analysis was performed by energy-dispersive X-ray spectroscopy. The chemical composition determined is consistent with graphene oxide The elements detected were carbon (50.31 at.%, atomic basis), oxygen (39.42 at.%), and small sulphur impurity (0.36 at.%). The oxygen signal can be attributed to the hydroxyl and carbonyl groups present in GO [24].

3.2. Adsorption of crystal violet on graphene oxide

3.2.1. Effect of contact time

To evaluate the effect of contact time, 3 mg of GO was added to a CV dye solution having different concentrations

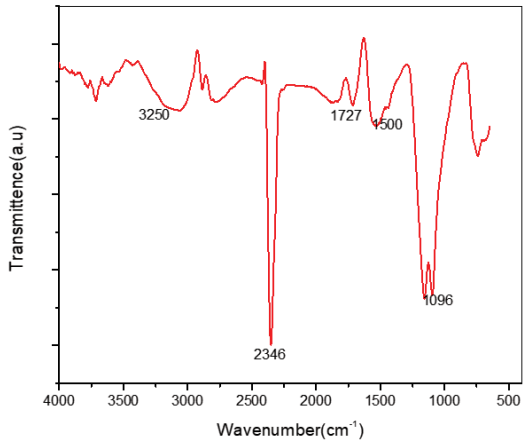

Fig. 1. Infrared spectrum of graphene oxide.

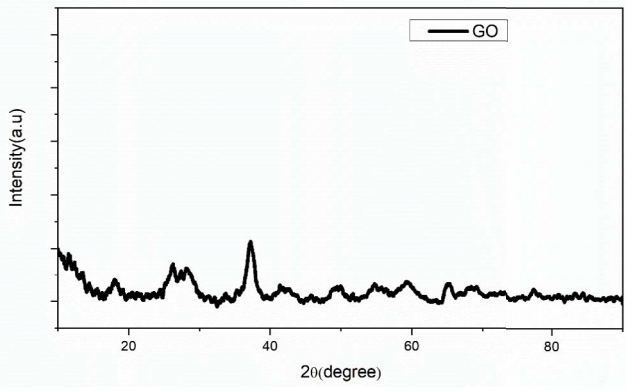

Fig. 2. X-ray diffraction of graphene oxide.

(2–6 ppm) and absorbance was recorded at different time intervals. The equilibrium time (the time required to achieve adsorption equilibrium), was determined to be 12 h. The percent dye adsorbed was determined as a function of time keeping all other parameters fixed. The result is shown in Fig. 4. As expected, it was observed that the extent of removal of crystal violet dye increases with increasing contact time because initially many vacant sites would be present at the surface but over time most of the vacant sites became occupied by CV [21]. When the initial concentration of the dye increased from 2–6 ppm, the percent removal of dye also increases up to 80%–90% after 24 h of the adsorption process.

3.2.2. Effect of adsorbent dose on adsorption of crystal violet onto graphene oxide

The impact of the adsorbent dose on the CV was examined by varying the amount of adsorbent in the range of 5 to 20 mg. It is observed that the removal of the dye increased as the amount of graphene oxide increased (Fig. 5). The removal capacity increases with an increase in adsorbent dose because as the amount of adsorbent is increased from 5 to 20 mg there is an increase in surface area and the number of adsorption sites available because of which dye removal efficiency of the graphene oxide increases [27].

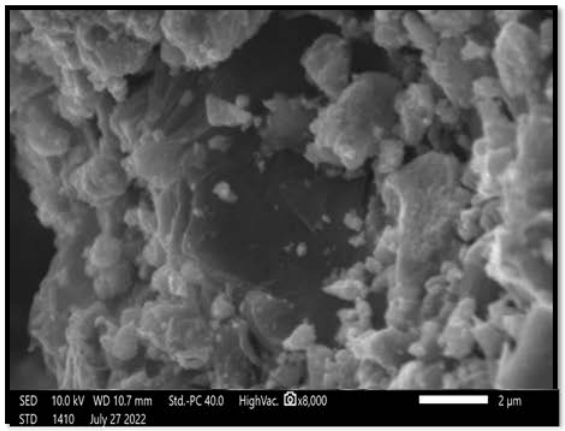

Fig. 3. Scanning electron microscopy of graphene oxide.

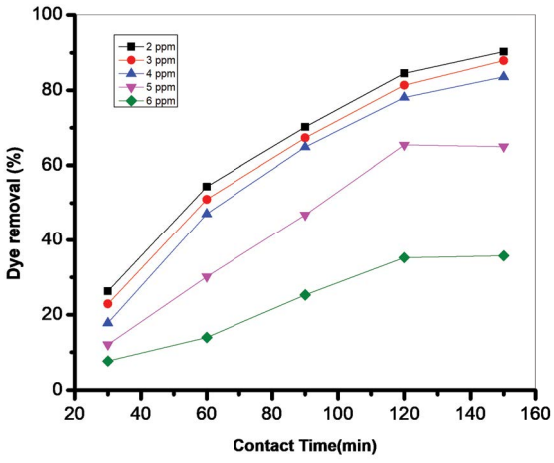

Fig. 4. Effect of contact time on different concentration of crystal violet.

3.2.3. Effect of pH

To study the effect of the pH of dye solution on adsorptive behaviour experiments were carried out at different pH values in the range from 5 to 9 with a fixed initial dye concentration of 6 mg/L and with 3 mg of adsorbent. The results are depicted in Fig. 6 indicating that removal of the dye is greater at pH 9. It is observed, therefore, that graphene oxide exhibits high adsorption in basic medium and there is a decrease in adsorption capacity at lower pH. On increasing pH, the surface of GO becomes more negative. The electrostatic force of attraction between the GO surface and

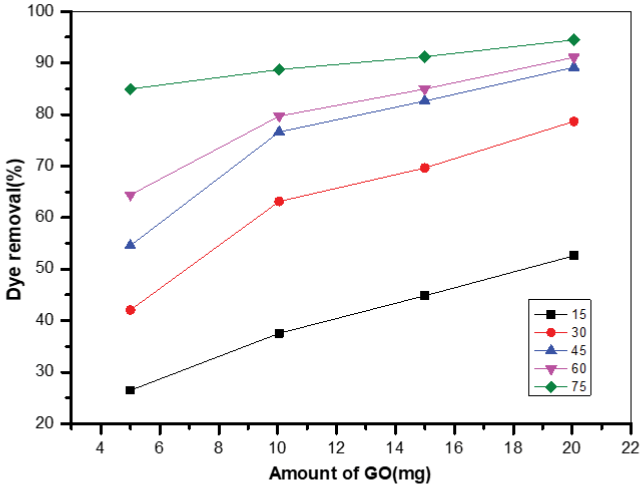

Fig. 5. Effect of dose of graphene oxide on % removal of crystal violet at different time interval.

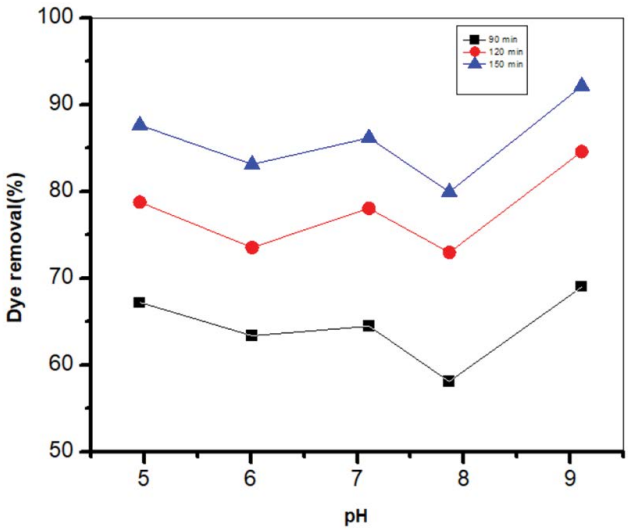

Fig. 6. Effect of pH of dye solution on % removal of crystal violet at different time interval.

CV would be expected to increase and this would enhance the adsorption of the positively charged CV [28]. Similar observations have been reported by Abd-Elhamid et al. [28].

3.2.4. Effect of temperature

The effect of temperature on dye removal was investigated in the range of 298 to 313 K and the results are shown in Fig. 7. It is observed that the percentage removal of dye and the amount of dye uptake increase with an increase in temperature. This indicates the favourability of dye adsorption at higher temperatures [29,30]. As the temperature increases, the dye molecules diffuse more quickly which results in a greater chance to encounter specific sites. When the temperature ascends, the viscosity of the dye solution decreases so there is also an increase in the rate of diffusion of dye molecules across the external boundary. With the increase in temperature molecules also have more energy to overcome the activation energy barrier to adsorption.

4. Adsorption isotherms

Various adsorption isotherms are used to study the interaction of adsorbents with dyes. Herein, Freundlich, Langmuir and Temkin isotherm models are used to analyze the interaction between crystal violet and graphene oxide. In the Freundlich adsorption isotherm, the adsorbate forms a multilayer on the heterogenous surface of the adsorbent that has different affinities. The Langmuir adsorption isotherm is based on the adsorption of dye molecules onto a homogeneous surface and maximum adsorption occurs when the surface is completely covered. The Temkin model assumes that the heat of the adsorption of all molecules decreases linearly with an increase. The linear forms of Freundlich, Langmuir and Temkin isotherms are given in Eqs. (9)–(11) [22,31–33].

$$\text{Freundlich isotherm}: \ln Q_e = \ln K_f + \frac{1}{n}\log C_e \tag{9}$$

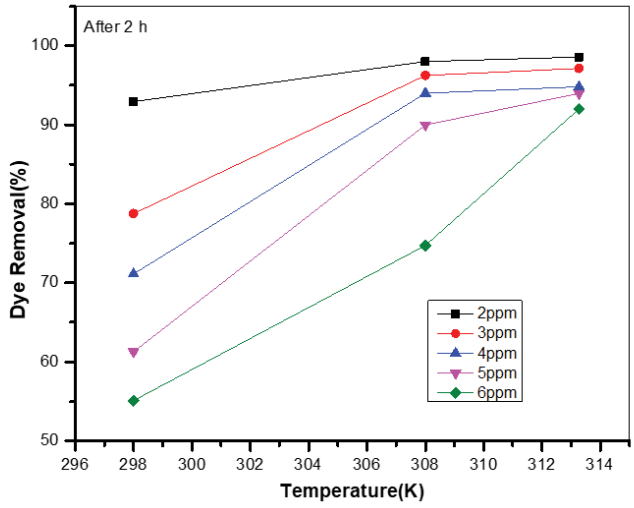

Fig. 7. Effect of temperature on different concentration of crystal violet.

$$\text{Langmuir isotherm}: \frac{C_e}{Q_e} = \frac{1}{K_L}\frac{1}{Q_L} + \frac{C_e}{Q_L} \tag{10}$$

$$\text{Temkin isotherm}: Q_e = \frac{RT}{b_T}\ln K_T + \frac{RT}{b_T}\ln C_e \tag{11}$$

where Q_e (mg/g) is the amount of adsorbate adsorbed by an adsorbent at equilibrium, C_e (mg/L) is the equilibrium concentration of the dye solution. K_f and n, K_L and Q_L, b_T and K_T are empirical constants incorporating all parameters affecting the adsorption process for Freundlich, Langmuir, and Temkin adsorption isotherms, respectively. R is the gas constant (8.314 J/mol·K) and T is the temperature (K). K_f and $1/n$ denote the adsorption capacity and adsorption intensity (surface heterogeneity), respectively in the Freundlich isotherm. Likewise, Q_L and K_L in the Langmuir isotherm denote adsorption capacity and energy adsorption. In the Temkin isotherm, K_T is related to the equilibrium binding energy and b_T is the Temkin constant related to the heat of adsorption and B is the adsorption-free energy and ε is the Polanyi potential.

The adsorption isotherm fits of graphene oxide are shown in Fig. 8a–d and parameters for the same are listed in Table 1. The relationship between the remaining dye concentration in solution (C_e) and the amount of dye adsorbed (Q_e) is shown in Fig. 8d. Among these three adsorption isotherms, the Temkin isotherm gives the best fit for the present work. According to the coefficient of determination (R^2). In the adsorption process, R^2 is the number indicating the proportion of the variance in the dependent variable which is predictable from the independent variable. In Table 1 we have reported the value of R^2 for various isotherms. It is observed that Temkin isotherm is best fitted with an R^2 value of 0.94 for the sorption process. In the Freundlich isotherm, the intercept on the X-axis is K_f which has a value here of 2.7 and the gradient gives $1/n$. The value of n is approximately equal to 1 which shows the process of adsorption is favourable at higher dye concentrations. The Langmuir isotherm generally gives information about the level of interaction between adsorbent and adsorbate. The higher value of K (496) indicates a strong interaction between crystal violet and graphene oxide.

5. Thermodynamic study

The thermodynamic study of the adsorption process was carried out at different temperatures in a thermostat water bath [30]. The thermodynamic parameters help us to determine the spontaneity of the adsorption process. The parameters viz. free energy (G), enthalpy (H) and entropy (S) for the adsorption of the dye by graphene oxide have been calculated using the following equations [34–36].

$$\frac{Q_e}{C_e} = \frac{\Delta S}{R} - \frac{\Delta H}{RT} \tag{12}$$

$$\Delta G = \Delta H - T\Delta S \tag{13}$$

where ΔS (kJ/mol·K), ΔH (kJ/mol), and ΔG (kJ/mol) are changes in entropy, enthalpy, and Gibb's free energy,

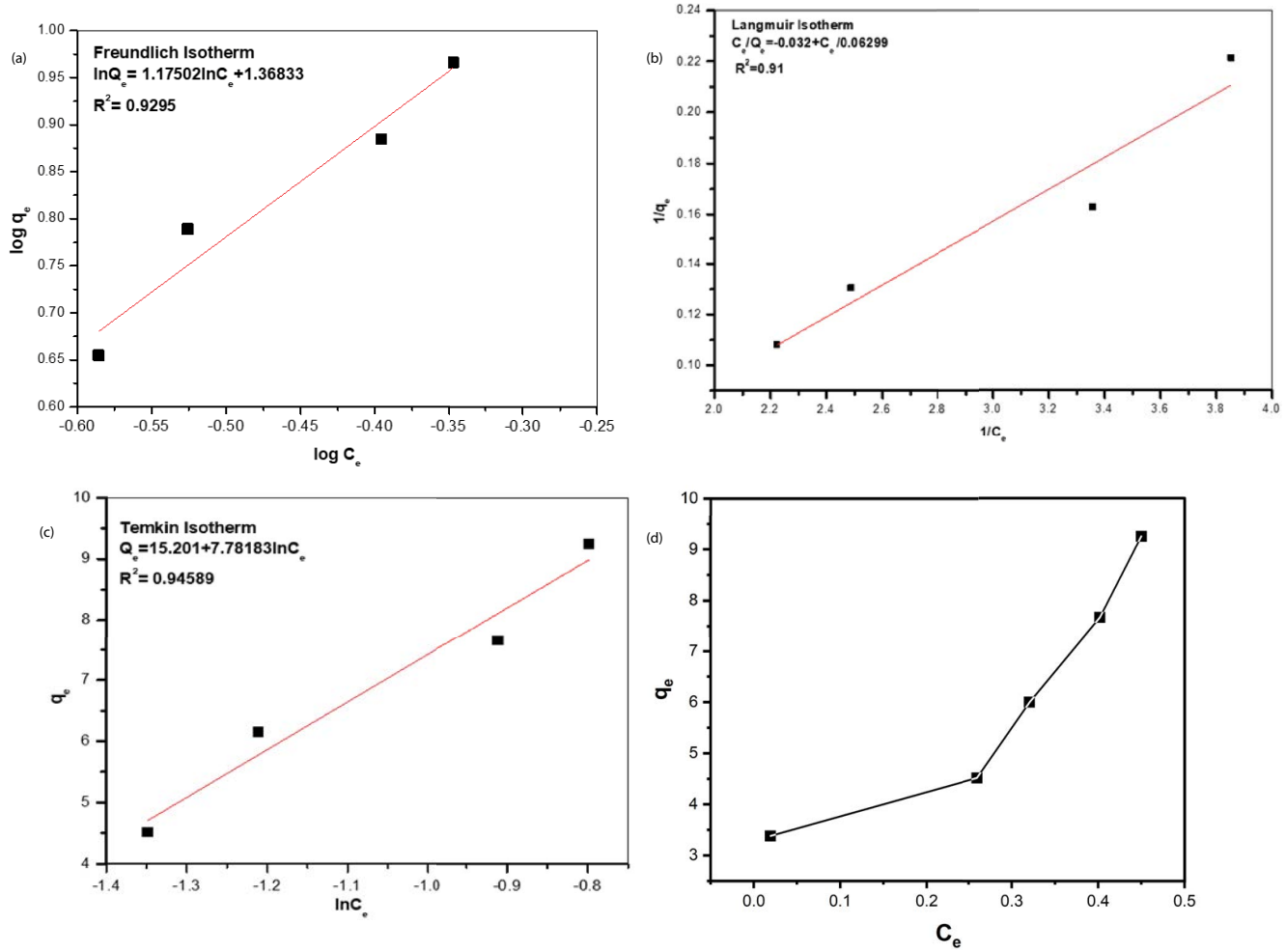

Fig. 8. Linear plot for (a) Freundlich isotherm, (b) Langmuir isotherm, (c) Temkin isotherm and (d) C_e vs. Q_e.

Table 1
Isotherm parameters

Concentration of dye (mg/L)		Q_e (mg/g)	Freundlich isotherm			Langmuir isotherm			Temkin isotherm		
Initial	C_e		n	K_f	R^2	Q_L	K_L	R^2	b_T	K_T	R^2
2	0.01	3.38									
3	0.26	4.52									
4	0.29	6.15	0.571	2.7	0.93	15.87	496.03	0.91	329.063	7.055	0.94
5	0.40	7.66									
6	0.45	9.25									

respectively. C_e is the equilibrium concentration (mg/L) of dye solution, Q_e is the amount of dye adsorbed at equilibrium (mg/g), R is the gas constant (8.314 J/mol·K) and T is the temperature (K). In Fig. 9 the slope of the plot of $\ln(Q_e/C_e)$ vs $1/T$ gives the value of ΔS and ΔH from its slope ($\Delta H/R$) and intercept ($\Delta S/R$). The ΔG value can be calculated using Eq. (13). The value of thermodynamics parameters is shown in Table 2. The enthalpies of adsorption are negative which shows the exothermic nature of adsorption. The change in free energy (ΔG) was negative, showing that the adsorption process is spontaneous in nature. The ΔG value became more negative with the increase in the temperature which indicates that adsorption was increasingly favoured at higher temperatures. The positive value of ΔS shows an increase in disorder which suggest that the dye molecules are randomly adsorbed onto the adsorbent surface.

6. Kinetic study

To examine the kinetics of the adsorption process such as chemical reaction, diffusion control, and mass transfer [37,38], several kinetics models are used to test the

experimental data. Three kinetic models were applied to understand the mechanism of dye adsorption. Pseudo-first-order, pseudo-second-order, and intraparticle diffusion models were used to identify the rate-governing steps in the adsorption process. The linear forms of these three models are expressed as Eqs. (14)–(16), respectively.

$$\text{Pseudo-first-order kinetics}: \ln\left(Q_e - Q_t\right) = \ln Q_e - K_1 t \quad (14)$$

$$\text{Pseudo-second-order kinetics} = \frac{t}{Q_e} + \frac{1}{K_2 Q_e^2} \quad (15)$$

$$\text{Interparticle diffusion}: Q_t = K_i t^{1/2} + C \quad (16)$$

where Q_t (mg/g) and Q_e (mg/g) are the amount of dye adsorbed at time t (min) and equilibrium, respectively and K_1 (min^{-1}), K_2 (g/mg·min), K_i (mg/g·min$^{1/2}$) are rate constants of adsorption for pseudo-first-order, pseudo-second-order and intraparticle diffusion, respectively. The intraparticle diffusion constant C reflects the boundary layer effect [39].

The linear plots for the kinetic models are shown in Fig. 10a–c and the constraints are enumerated in Table 3. It was found that the calculated value of adsorption capacity $q_{e,\text{cal}}$ (mg/g) was in better agreement with the experimental values $q_{e,\text{exp}}$, (mg/g) with a correlation coefficient ($R^2 > 0.9$). Hence, the pseudo-second-order kinetics model is best followed in the present study for all concentrations. The applicability of second-order kinetics suggests that the chemical reaction is responsible for the adsorption of crystal violet on graphene oxide. The study shows that intraparticle diffusion is precisely fitted for the current experiment. The value of constant C delivers information about the thickness of the boundary layer and the resistance to external mass transfer [40,41].

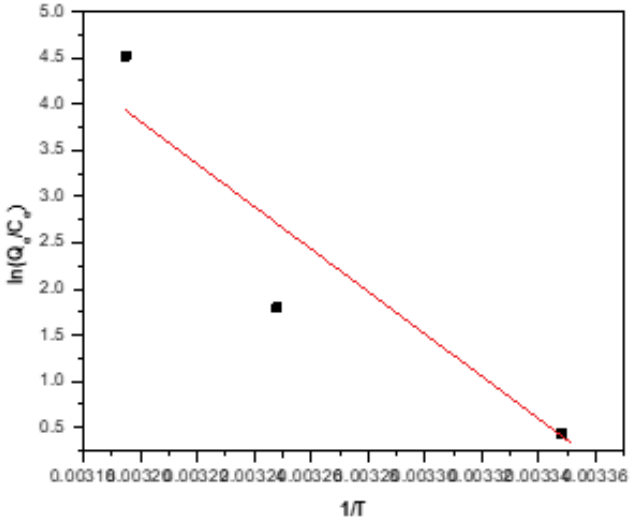

Fig. 9. Plot of $\ln(Q_e/C_e)$ vs. $1/T$ to give thermodynamics parameters.

7. Column procedure for removal of CV dye

While column experiment was carried out to test the practical utility of the prepared adsorbent. A static bed column trial was also carried out to study the removal of the CV dye using GO. A complicated breakthrough curve was obtained for the adsorption of CV dye on GO (Fig. 11). At first, many surface-active sites were available and the dye could be removed completely. Therefore, the value of C_t/C_0 obtained equal to zero during the initial 15 min. After that a different phenomenon occurs and values increase slightly. This increase continued over time and a *S*-shaped breakthrough curve was obtained. The breakthrough and exhaustion point were observed at C_e/C_0 being approximately at 0.032 and at 0.43, respectively after passing dye solution through the column. The area under the curve is found to be 4,701 cm^2. The total amount of dye adsorbed through column is found to be 11.7 mL/cm^2·min [42,43].

8. Cost estimation

In India, the cheapest variety of graphite powder available is Rs. 500/kg. The other chemical which are used in preparation of graphene oxide like $KMnO_4$, H_2O_2, H_2SO_4, and $NaNO_3$ are used in very small quantity and cost per kg is Rs. 160–190, 160/L, Rs. 15/L and Rs. 95/kg, respectively. When

Table 2
Thermodynamics parameter

Concentration (mg/L)	ΔH (kJ/mol)	ΔS (kJ/mol·K)	ΔG (kJ/mol) at temperature		
			298 K	308 K	313 K
5	–191.15	0.643	–0.459	–6.89	–10.10

Table 3
Kinetics parameter for adsorption of crystal violet on graphene oxide

Concentration of dye (mg/L)	Q_e (mg/g)	Pseudo-first-order			Pseudo-second-order			Intraparticle		
		Q_e	K_1	R^2	Q_e	K_2	R^2	K_i	C	R^2
2	3.38	2.65	0.025	0.89	4.08	2.16	0.98	0.21		0.83
3	4.51	14.43	0.042	0.89	5.69	5.15	0.98	0.29		0.82
4	6.15	21.67	0.040	0.89	9.17	10.47	0.99	0.51		0.98
5	7.66	168.24	0.066	0.89	11.14	16.22	0.89	0.61		0.95
6	9.25	43.68	0.045	0.59	11.97	33.52	0.98	0.64		0.99

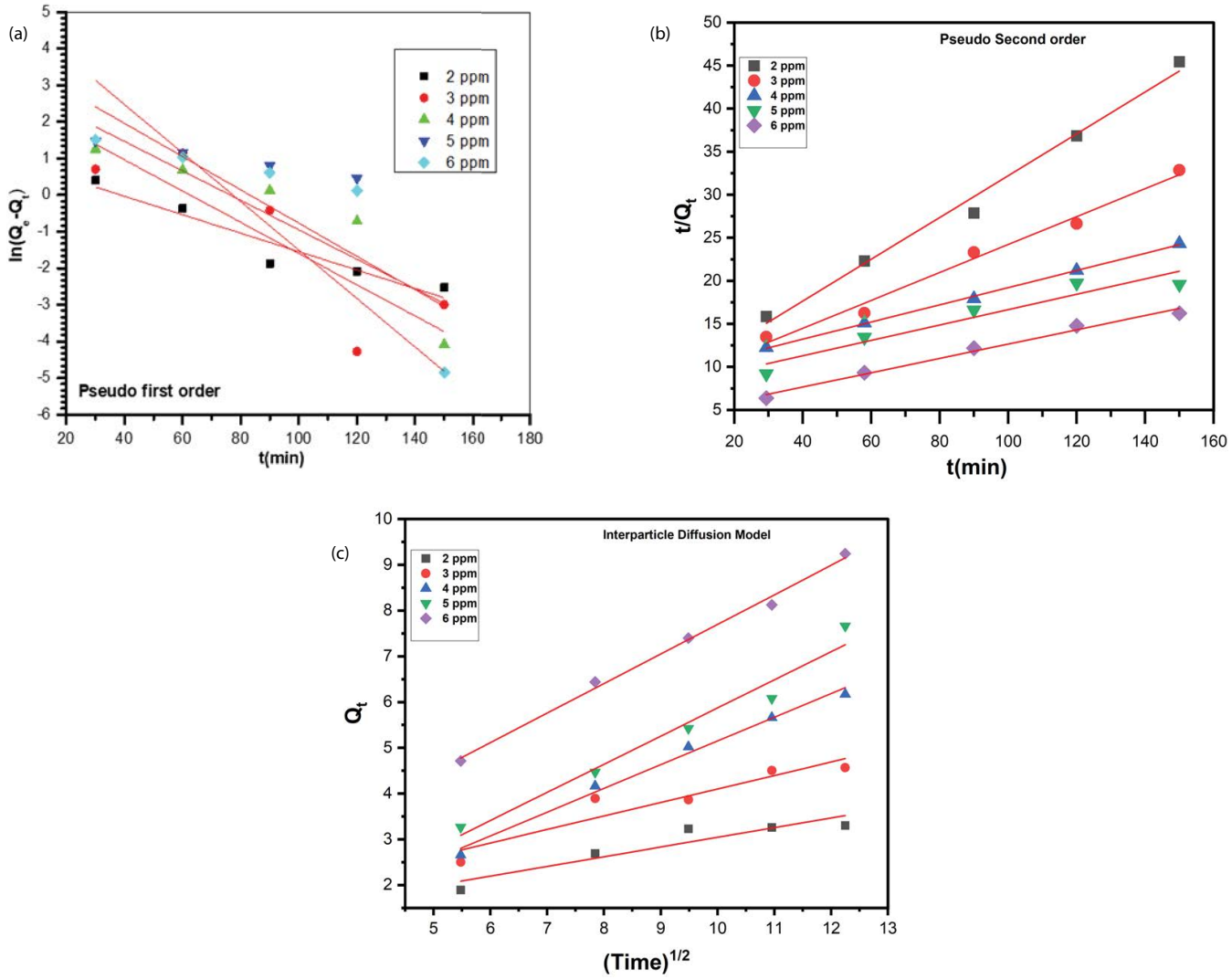

Fig. 10. Linear plot for (a) pseudo-first-order reaction, (b) pseudo-second-order reaction and (c) intraparticle diffusion.

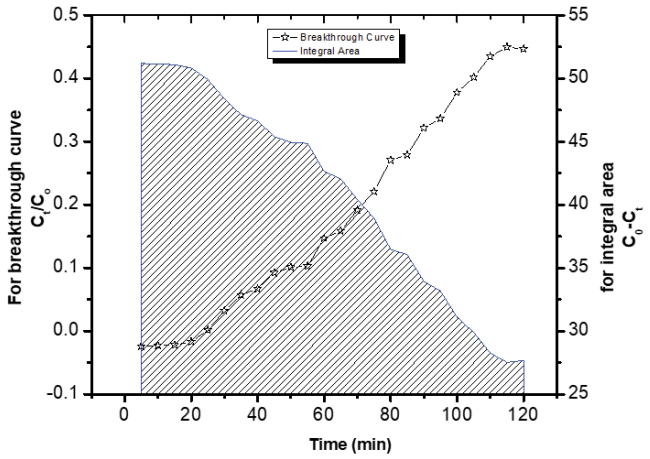

Fig. 11. Breakthrough curve (line, left vertical axis) and integral area (shaded, right vertical axis) of crystal violet on graphene oxide in a fixed bed column experiment.

the total cost for transport, chemicals, electrical energy, etc. are added up, the finished product would cost approximately Rs. 2,500/kg. The adsorbent material can be chemically regenerated and reused which can further bring down the cost. Besides, the cost was estimated at laboratory scale preparation of adsorbent so it might be high but on industrial scale preparation the cost of preparation of adsorbent would further decrease as the chemicals would be ordered in bulk at much lower price.

9. Conclusion

It has been demonstrated that graphene oxide can be used as an efficient potential adsorbent for CV. Its adsorption capacity was studied in detail varying the parameters of contact time, adsorbent dose, pH, temperature, and initial dye concentration. The maximum adsorption of dye was recorded at 313 K for the 2-ppm solution. The H^+ ion in the acidic medium is found to inhibit the adsorption, hence the greater adsorption of CV on graphene oxide is recorded in

the basic medium with a maximum removal efficiency of 92% at the highest pH studied of pH = 9. The adsorption of CV dye was best fitted by the Temkin adsorption isotherm. From the kinetic study of the adsorption process, it is revealed that the adsorption process is exothermic in nature. Among the three kinetics models that were studied for CV dye, pseudo-second-order kinetics gave the best fit. This shows that adsorption proceeds via chemisorption. The thermodynamics parameters obtained indicate the adsorption to be spontaneous and favourable at the higher temperatures studied. Through column studies, it is found that GO is promising for application in the industry since it efficiently removes CV from 50 ppm solution in a few hours. Hence, we can conclude that graphene oxide is an efficient and economical adsorbent for crystal violet.

Acknowledgment

One of the authors NR is thankful to University Grants Commission, New Delhi, India for providing VRET Fellowship for pursuing Ph.D. XRD and SEM were performed at the School of Chemistry, University of St. Andrews. The Electron Microscopy Facility at St. Andrews is supported by the Engineering and Physical Science Research Council of the UK (grants EP/L017008/1, EP/R023751/1, and EP/T019298/1).

References

[1] S. Jayanthi, N.K. Eswar, S.A. Singh, K. Chatterjee, G. Madras, A.K. Sood, Macroporous three-dimensional graphene oxide foams for dye adsorption and antibacterial applications, RSC Adv., 6 (2016) 1231–1242.
[2] S.-Y. Mak, D.-H. Chen, Fast adsorption of methylene blue on polyacrylic acid-bound iron oxide magnetic nanoparticles, Dyes Pigm., 61 (2004) 93–98.
[3] W.J. Zhang, C.J. Zhou, W.C. Zhou, A.H. Lei, Q.L. Zhang, Q. Wan, B.S. Zou, Fast and considerable adsorption of methylene blue dye onto graphene oxide, Bull. Environ. Contam. Toxicol., 87 (2011) 86–90.
[4] V.K. Gupta, T.A. Saleh, Sorption of pollutants by porous carbon, carbon nanotubes and fullerene—an overview, Environ. Sci. Pollut. Res., 20 (2013) 2828–2843.
[5] C.D. Raman, S. Kanmani, Textile dye degradation using nano zero valent iron: a review, J. Environ. Manage., 177 (2016) 341–355.
[6] Mohd. Rafatullah, O. Sulaiman, R. Hashim, A. Ahmad, Adsorption of methylene blue on low-cost adsorbents: a review, J. Hazard. Mater., 177 (2010) 70–80.
[7] G. Mezohegyi, F.P. van der Zee, J. Font, A. Fortuny, A. Fabregat, Towards advanced aqueous dye removal processes: a short review on the versatile role of activated carbon, J. Environ. Manage., 102 (2012) 148–164.
[8] M.N. Khan, O. Bashir, T.A. Khan, S.A. Al-Thabaiti, Z. Khan, Catalytic activity of cobalt nanoparticles for dye and 4-nitro phenol degradation: a kinetic and mechanistic study, Int. J. Chem. Kinet., 49 (2017) 438–454.
[9] A. Gupta, S.A. Khan, T.A. Khan, Chapter 11 – Remediation of Textile Wastewater by Ozonation, L.J. Rather, M. Shabbir, A. Haji, Eds., Sustainable Practices in the Textile Industry, Wiley, New Jersey, USA, 2021, pp. 273–284. Available at: https://doi.org/10.1002/9781119818915.ch11
[10] V.K. Gupta, Suhas, Application of low-cost adsorbents for dye removal – a review, J. Environ. Manage., 90 (2009) 2313–2342.
[11] L. Bulgariu, L.B. Escudero, O.S. Bello, M. Iqbal, J. Nisar, K.A. Adegoke, F. Alakhras, M. Kornaros, I. Anastopoulos, The utilization of leaf-based adsorbents for dyes removal: a review, J. Mol. Liq., 276 (2019) 728–747.
[12] A. Kausar, M. Iqbal, A. Javed, K. Aftab, Zill-i-Huma Nazli, H.N. Bhatti, S. Nouren, Dyes adsorption using clay and modified clay: a review, J. Mol. Liq., 256 (2018) 395–407.
[13] A. Anastopoulos, A. Hosseini-Bandegharaei, J. Fu, A.C. Mitropoulos, G.Z. Kyzas, Use of nanoparticles for dye adsorption: review, J. Dispersion Sci. Technol., 39 (2017) 836–847.
[14] A. Bhatnagar, M. Sillanpää, A. Witek-Krowiak, Agricultural waste peels as versatile biomass for water purification – a review, Chem. Eng. J., 270 (2015) 244–271.
[15] A.K. Geim, K.S. Novoselov, The rise of graphene, Nat. Mater., 6 (2007) 183–191.
[16] I.W. Frank, D.M. Tanenbaum, A.M. van der Zande, P.L. McEuen, Mechanical properties of suspended graphene sheets, J. Vac. Sci. Technol., B, 25 (2007) 2558–2561.
[17] A.A. Balandin, S. Ghosh, W. Bao, I. Calizo, D. Teweldebrhan, F. Miao, C.N. Lau, Superior thermal conductivity of single-layer graphene, Nano Lett., 8 (2008) 902–907.
[18] W.S. Hummers Jr., R.E. Offeman, Preparation of graphitic oxide, J. Am. Chem. Soc., 80 (1958) 1339, doi: 10.1021/ja01539a017.
[19] A.E. Khan, Shahjahan, T.A. Khan, Synthesis of magnetic iron-manganese oxide coated graphene oxide and its application for adsorptive removal of basic dyes from aqueous solution: isotherm, kinetics, and thermodynamic studies, Environ. Prog. Sustainable Energy, 38 (2019) S214–S229.
[20] T.A. Khan, M. Nazir, E.A. Khan, Magnetically modified multiwalled carbon nanotubes for the adsorption of bismarck brown R and Cd(II) from aqueous solution: batch and column studies, Desal. Water Treat., 57 (2016) 19374–19390.
[21] C. Arora, P. Kumar, S. Soni, J. Mittal, A. Mittal, B. Singh, Efficient removal of malachite green dye from aqueous solution using *Curcuma caesia* based activated carbon, Desal. Water Treat., 195 (2020) 341–352.
[22] S. Soni, P.K. Bajpai, Mittal, C. Arora, Utilisation of cobalt doped Iron based MOF for enhanced removal and recovery of methylene blue dye from wastewater, J. Mol. Liq., 314 (2020) 113642, doi: 10.1016/j.molliq.2020.113642.
[23] S. Soni, N. Rai, P.K. Bajpai, J. Mittal, C. Arora, Enhanced sequestration of an acidic dye on novel bimetallic metal-organic framework, J. Dispersion Sci. Technol., (2022), doi: 10.1080/01932691.2022.2135521.
[24] G.C. Mohan Kumar, M. Jalageri, Synthesis and characterization of graphene oxide by modified hummer method, AIP Conf. Proc., 2247 (2020) 040018, doi: 10.1063/5.0003864.
[25] W. Chen, L. Yan, P.R. Bangal, Preparation of graphene by the rapid and mild thermal reduction of graphene oxide induced by microwaves, Carbon, 48 (2010) 1146–1152.
[26] S. Jianguo, X. Wang, C.-T. Chang, Preparation and characterization of graphene oxide, J. Nanomater., 2014 (2014) 276143, doi: 10.1155/2014/276143.
[27] H. Guo, F. Lin, J. Chen, F. Li, W. Weng, Metal–organic framework MIL-125(Ti) for efficient adsorptive removal of Rhodamine B from aqueous solution, Appl. Organomet. Chem., 29 (2015) 12–19.
[28] A.L. Abd-Elhamid, H.F. Aly, H.A.M. Soliman, A.A. El-Shanshory, Graphene oxide: follow the oxidation mechanism and its application in water treatment, J. Mol. Liq., 265 (2018) 226–237.
[29] A. Mittal, J. Mittal, A. Malviya, D. Kaur, V.K. Gupta, Decoloration treatment of a hazardous triarylmethane dye, Light Green SF (Yellowish) by waste material adsorbents, J. Colloid Interface Sci., 342 (2010) 518–527.
[30] Y. Xu, J. Jin, X. Li, Y. Han, H. Meng, C. Song, X. Zhang, Magnetization of a Cu(II)-1,3,5-benzenetricarboxylate metal-organic framework for efficient solid-phase extraction of Congo red, Microchim. Acta, 182 (2015) 2313–2320.
[31] C. Arora, S. Soni, S. Sahu, J. Mittal, P. Kumar, P.K. Bajpai, Iron based metal organic framework for efficient removal of methylene blue dye from industrial waste, J. Mol. Liq., 284 (2019) 343–352.
[32] A.K. Kushwaha, N. Gupta, M.C. Chattopadhyaya, Removal of cationic methylene blue and malachite green dyes from aqueous solution by waste materials of *Daucus carota*, J. Saudi Chem. Soc., 18 (2014) 200–207.

[33] A. Mittal, J. Mittal, A. Malviya, D. Kaur, V.K. Gupta, Decoloration treatment of a hazardous triarylmethane dye, Light Green SF (Yellowish) by waste material adsorbents, J. Colloid Interface Sci., 342 (2010) 518–527.
[34] N. Abbasi, S.A. Khan, T.A. Khan, Response surface methodology mediated process optimization of Celestine blue B uptake by novel custard apple seeds activated carbon/$FeMoO_4$ nanocomposite, J. Water Process Eng., 43 (2021) 102267, doi: 10.1016/j.jwpe.2021.102267.
[35] P. Senthil Kumar, M. Palaniyappan, M. Priyadharshini, A.M. Vignesh, A. Thanjiappan, P. Sebastina Anne Fernando, R. Tanvir Ahmed, R. Srinath, Adsorption of basic dye onto raw and surface-modified agricultural waste, Environ. Prog. Sustainable Energy, 33 (2014) 87–98.
[36] A.R. Tehrani-Bagha, H. Nikkar, N.M. Mahmoodi, M. Markazi, F.M. Menger, The sorption of cationic dyes onto kaolin: kinetic, isotherm and thermodynamic studies, Desalination, 266 (2011) 274–280.
[37] S. Wu, J. Huang, C. Zhuo, F. Zhang, W. Sheng, M. Zhu, One-step fabrication of magnetic carbon nanocomposite as adsorbent for removal of methylene blue, J. Inorg. Organomet. Polym. Mater., 26 (2016) 632–639.
[38] A.A. Mohammadi, A. Alinejad, B. Kamarehie, S. Javan, A. Ghaderpoury, M. Ahmadpour, M. Ghaderpoori, Metal-organic framework Uio-66 for adsorption of methylene blue dye from aqueous solutions, Int. J. Environ. Sci. Technol., 14 (2017) 1959–1968.
[39] M.T. Yagub, T.K. Sen, H.M. Ang, Equilibrium, kinetics, and thermodynamics of methylene blue adsorption by pine tree leaves, Water Air Soil Pollut., 223 (2012) 5267–5282.
[40] S.A. Umoren, U.J. Etim, A.U. Israel, Adsorption of methylene blue from industrial effluent using poly(vinyl alcohol), J. Mater. Environ. Sci., 4 (2013) 75–86.
[41] C. Li, X. Wang, D. Meng, L. Zhou, Facile synthesis of low-cost magnetic biosorbent from peach gum polysaccharide for selective and efficient removal of cationic dyes, Int. J. Biol. Macromol., 107 (2018) 1871–1878.
[42] L. Zhang, D. Zhao, Y. Lu, J. Chen, H. Li, J. Xie, Y. Xu, H. Yuan, X. Liu, X. Zhu, J. Lu, A graphene oxide modified cellulose nanocrystal/PNIPAAm IPN hydrogel for the adsorption of Congo red and methylene blue, New J. Chem., 45 (2021) 16679–16688.
[43] M.S. Mansour, M.E. Ossman, H.A. Farag, Removal of Cd(II) ion from waste water by adsorption onto polyaniline coated on sawdust. Desalination, 272 (2011) 301–305.